

Packet-Level Index Modulation Based on Channel Activity Detection

Kosuke Suzuki¹, Member, IEEE, Koichi Adachi², Senior Member, IEEE, Mai Ohta, Member, IEEE, Osamu Takyu³, Member, IEEE, and Takeo Fujii⁴, Senior Member, IEEE

Abstract—In recent years, long-range wide-area network (LoRaWAN) has attracted considerable attention due to its ability to realize massive machine-type communication (MTC); however, its throughput is limited by the duty cycle (DC). Packet-level index modulation (PLIM) can increase throughput by utilizing a data packet's frequency channel and transmission timing as the information-bearing index. In PLIM, a node selects a specific transmission resource (frequency channel and timing) within a frame and transmits a packet. If the node cannot transmit the packet at the specific transmission resource, it discards the packet. This packet discard results in throughput degradation of each node. Thus, this paper proposes an index mapping scheme that divides a frame into multiple subframes to provide each node with multiple transmission opportunities. A node performs channel activity detection (CAD) at the selected transmission resource within a subframe; if the node cannot transmit a packet, it moves to the next subframe. The proposed scheme adaptively maps the information bit sequence onto a transmission resource within each subframe based on the wireless environment and communication quality. Computer simulation results show that the proposed scheme improves throughput by increasing the transmission opportunities and reducing the packet discard rate under the constraint of DC.

Index Terms—Carrier sense, channel activity detection, LPWAN, LoRaWAN, index modulation.

I. INTRODUCTION

THE rapid development of the Internet-of-things (IoT) has stimulated the utilization of wireless sensor networks (WSN) in various applications [1], [2], [3], including industry [4] and healthcare [5]. In particular, low-power wide-area networks (LPWANs) that enable massive machine-type communication (MTC) have attracted considerable attention [6], [7], [8]. When many end nodes (ENs) share limited

wireless resources to communicate with a single gateway (GW) and send data packets simultaneously on the same frequency channel, the GW may not be able to receive data correctly. For fair frequency sharing, LPWAN specifies a maximum time duration for each node, including GWs, to use a particular frequency channel [9]; it is called a duty cycle (DC). Thus, nodes cannot increase the number of transmitted packets to increase the amount of data.

Among all available LPWAN standards, long-range wide-area network (LoRaWAN) has attracted the most attention since it specifies an open standard [10] and allows construction of autonomous LPWAN networks [11]. LoRaWAN uses chirp spread spectrum (CSS) modulation in the physical (PHY) layer to achieve long-range communication with low power consumption. The number of bits transmitted in one symbol, called spreading factor (SF), is a parameter of CSS modulation and can be set in the range of 7 to 12 [12]. Increasing the SF improves noise immunity but reduces the transmission rate. To reduce power consumption, LoRaWAN uses the ALOHA protocol in the medium access control (MAC) layer and does not perform carrier sense multiple access/collision avoidance (CSMA/CA) or listen before talk (LBT). Thus, packet collisions cannot be avoided in environments where thousands of ENs are connected to the network [13]. To avoid packet collision, an EN can perform carrier sensing (CS) before packet transmission to sense the transmission status of other ENs. CS helps detect the ongoing transmission of other ENs based on the received signal strength (RSS) over the entire bandwidth of the transmitted signal. However, CS may not be able to detect CSS-modulated LoRa signals even if there are any because the signal power may become lower than the noise floor level due to spreading [14].

As an alternative to CS, the LoRaWAN chip has a sensing function called *channel activity detection (CAD)* [14]. An EN locally generates chirp signals with the same SF on its own and cross-correlates them with the received signal on the frequency channel on which it will transmit a packet. Therefore, the EN can detect LoRa signals on its own transmit frequency channel and SF with low power consumption and high accuracy. However, it cannot detect LoRa signals with SF different from its own or signals other than LoRa. Although CAD is designed to detect preambles of LoRa packets, it can detect signals more than 95% of the transmission time, including the payload part [15]. In addition, experiments have shown that the preamble and payload of the LoRa signal can be detected at distances of more than 4 km from the detecting node [16]. Therefore, numerous methods have been pro-

Manuscript received 30 November 2022; revised 1 June 2023; accepted 30 July 2023. Date of publication 14 August 2023; date of current version 11 April 2024. This work was supported by the Ministry of Internal Affairs and Communications (MIC)/Strategic Information and Communications Research and Development Promotion Programme (SCOPE) under Grant JP205004001. The associate editor coordinating the review of this article and approving it for publication was X. Cheng. (Corresponding author: Kosuke Suzuki.)

Kosuke Suzuki, Koichi Adachi, and Takeo Fujii are with the Advanced Wireless and Communication Research Center (AWCC), The University of Electro-Communications, Chofu, Tokyo 182-8585, Japan (e-mail: suzuki@awcc.uec.ac.jp).

Mai Ohta is with the Department of Electronics Engineering and Computer Science, Faculty of Engineering, Fukuoka University, Jonan, Fukuoka 814-018, Japan.

Osamu Takyu is with the Department of Electrical and Computer Engineering, Faculty of Engineering, Shinshu University, Wakasato, Nagano 380-8553, Japan.

Color versions of one or more figures in this article are available at <https://doi.org/10.1109/TWC.2023.3303187>.

Digital Object Identifier 10.1109/TWC.2023.3303187

posed and evaluated to realize CSMA/CA and LBT using CAD [15], [17], [18], [19], [20], [21], [22], [23]. CSMA/CA and LBT can significantly lower the packet collision rate and improve the packet delivery rate (PDR) of LoRaWAN at the cost of a slight increase in energy consumption at each EN.

There are two types of packets in LoRaWAN: *confirmed (CONF) packets* and *unconfirmed (UNC) packets* [10]. The packet type is assigned as message type (MType) in the first 3 bits of the MAC header in a LoRaWAN packet. The GW determines the packet type by referring to the corresponding bits after demodulating the packet. If it receives a UNC packet from the EN, the GW does not send an ACK packet. However, if it receives a CONF packet, it sends an ACK packet to the EN after a certain period of time. The GW sends the first ACK packet to the EN $RECEIVE_DELAY_1$ [sec] after receiving the CONF packet and sends the second ACK packet to the EN after $RECEIVE_DELAY_2$ [sec] [10]. If an EN sends a CONF packet but does not receive an ACK, it retransmits the packet. Packet retransmission prevents the loss of transmitted data but incurs communication overhead due to ACK transmission. Furthermore, ACK transmission puts a strain on the DC of the GW. In low-traffic-load environments, packet retransmission prevents the loss of transmitted data and improves network performance. On the contrary, in environments with a high traffic load, packet retransmissions degrade network performance [24]. This is because when an EN sends a CONF packet and GW receives the packet successfully but cannot send an ACK packet due to DC constraints, the EN retransmits the packet despite successful packet transmission. In a WSN with multiple ENs transmitting data, individual data may not be so important; thus, CONF packets should be used appropriately as per system requirements [25].

While CAD and retransmission improve quality-of-service (QoS) by reducing packet discards and transmission failures, they cannot increase the amount of data transmitted. The authors previously proposed packet-level index modulation (PLIM), which focuses on periodically generated data in various situations, by adopting LoRaWAN [26]. PLIM is a type of index modulation (IM) scheme [27] that adds additional information to the combination of frequency channel and time slot (index) of transmitted packets to increase the bit rate without modifying the conventional LoRaWAN standard under DC constraints. Computer simulations show that the use of PLIM can increase the bit rate by up to 32.5% compared to conventional LoRaWAN. However, periodic packet collisions may occur when multiple ENs select the same PLIM bit sequence periodically. In addition, since frequency channels and time slots directly represent the PLIM bit sequence, the number of frequency channels and time slots must be an integer power of 2, and excess resources cannot be utilized.

To address the problems of PLIM [26], the authors proposed a flexible index mapping scheme [29]. This mapping scheme increases the number of bits transmitted by the index and avoids packet collisions by utilizing all available frequency channels and time slots when a prohibited frequency channel is given. Theoretical performance evaluation showed that the proposed scheme improves throughput performance by

approximately 18% compared to conventional PLIM [26] and significantly reduces the overhead between EN and GW. However, it was found that transmission efficiency may degrade because packets must be transmitted using specific resources (frequency channel and transmission timing) according to the bit sequence transmitted by PLIM. If CAD detects the signal of another EN before the packet is transmitted, the EN discards the packet, that is, each packet has only one opportunity to be transmitted.

Considering the above, this paper proposes an index mapping scheme that flexibly divides a frame into multiple subframes to provide multiple transmission opportunities for each packet and improve throughput under DC constraints. Specifically, the EN first divides the frame into multiple subframes. Next, it selects a transmission resource (frequency channel and time slot) in the first subframe, and CAD is performed before transmission begins. If the EN detects another EN's signal using CAD, it re-selects the transmission resource in the next subframe; however, if it does not, it transmits the packet. This process is repeated to give each packet multiple transmission opportunities and reduce the packet discard rate.

We describe the proposed scheme in two parts: (i) enhanced index mapper and de-mapper, and (ii) CAD-based PLIM. The remainder of this paper is organized as follows. An overview of PLIM and flexible index mapping is provided in Section II. Section III describes the enhanced index mapper and de-mapper, while CAD-based PLIM is described in Section IV. The computer simulation and its results are discussed in Section V. Finally, Section VI summarizes the paper.

II. PACKET-LEVEL INDEX MODULATION (PLIM)

A. Overview [26]

Without loss of generality, we consider the communication between one specific EN and the GW over K frequency channels. We assume that an EN generates data packets such as sensing information every T_{frame} [sec]. Frame length T_{frame} is split into Q non-overlapping time slots with equal time length of T_{slot} [sec]. Once the EN generates an information bit sequence $\mathbf{B} \in \{0, 1\}^{B \times 1}$ of length B [bits], it divides \mathbf{B} into payload bit sequence $\mathbf{B}_{\text{pl}} \in \{0, 1\}^{B_{\text{pl}} \times 1}$ and PLIM bit sequence $\mathbf{B}_{\text{plim}} \in \{0, 1\}^{B_{\text{plim}} \times 1}$. Here, B_{pl} and B_{plim} represent the payload bit sequence length and the PLIM bit sequence length, respectively, that is, $B_{\text{pl}} + B_{\text{plim}} = B$. The EN generates a data packet using \mathbf{B}_{pl} in the same manner as conventional LoRaWAN. Further, it transmits the generated data packet at frequency channel $k \in \mathcal{K} = \{0, 1, \dots, K-1\}$ and time slot $q \in \mathcal{Q} = \{0, 1, \dots, Q-1\}$, which are determined by

$$(k, q) = \mathcal{F}_{\text{plim}}(\mathbf{B}_{\text{plim}}), \quad (1)$$

where $\mathcal{F}_{\text{plim}}$ denotes an arbitrary index mapper.

Once the GW receives a packet on frequency channel $\tilde{k} \in \mathcal{K}$, it estimates time slot $\tilde{q} \in \mathcal{Q}$ [28]. The combination of the estimated frequency channel and time slots, (\tilde{k}, \tilde{q}) , are input to the index de-mapper $\mathcal{F}_{\text{plim}}^{-1}$, which demodulates the PLIM bit sequence $\tilde{\mathbf{B}}_{\text{plim}} \in \{0, 1\}^{B_{\text{plim}} \times 1}$ as

$$\tilde{\mathbf{B}}_{\text{plim}} = \mathcal{F}_{\text{plim}}^{-1}(\tilde{k}, \tilde{q}). \quad (2)$$

B. Flexible Index Mapping [29]

Flexible index mapping adaptively maps the index to all available resources to avoid packet collisions by increasing the number of bits transmitted in the index. Specifically, flexible index mapping proposes index mapper \mathcal{F}_{fim} and index de-mapper $\mathcal{F}_{\text{fim}}^{-1}$, which utilize device address \mathbf{B}_{addr} and packet counter \mathbf{B}_{pcnt} contained in the header of LoRaWAN packets [10]. The device address \mathbf{B}_{addr} is an EN-specific value expressed in 4 bytes, while packet counter \mathbf{B}_{pcnt} is a packet-specific value expressed in 2 bytes. Let us denote the available frequency channel set as $\mathcal{A} = \{a_0, a_1, \dots, a_k, \dots, a_{K-1}\}$, where $a_k \in \{0, 1\}$ is the state of frequency channel k . When frequency channel k is available, $a_k = 1$; otherwise, $a_k = 0$. The number of available frequency channels K_a can be expressed as $K_a = \sum_{k=0}^{K-1} a_k$ ($0 < K_a \leq K$). Further, the number of available resources R can be expressed as $R = K_a \times Q$.

The EN converts PLIM bit sequence \mathbf{B}_{plim} , device address \mathbf{B}_{addr} , and packet counter \mathbf{B}_{pcnt} to decimal numbers that are expressed as D_{plim} , D_{addr} , and D_{pcnt} , respectively. Then, the EN calculates transmission code X as

$$X = \text{mod}(D_{\text{plim}} + f(D_{\text{addr}}, D_{\text{pcnt}}), R), \quad (3)$$

where $\text{mod}(m, n)$ represents the modulo of $m \in \mathbb{N}$ by $n \in \mathbb{N} \setminus \{0\}$, which is defined as

$$\text{mod}(m, n) = m - \left(n \times \left\lfloor \frac{m}{n} \right\rfloor \right), \quad (4)$$

where $\lfloor \cdot \rfloor$ is the floor function. Since we have $0 \leq \text{mod}(m, n) < n$, it is applicable even when m, n is negative. $f(D_{\text{addr}}, D_{\text{pcnt}})$ is an arbitrary function uniquely determined by D_{addr} and D_{pcnt} . Finally, the EN obtains transmission index (k, q) from X as

$$(k, q) = \left(\left\lfloor \frac{X}{Q} \right\rfloor + \sum_{k=0}^{\lfloor X/Q \rfloor} (1 - a_k), \text{mod}(X, Q) \right). \quad (5)$$

The EN transmits the data packet at frequency channel k and time slot q .

When the GW receives a data packet at frequency channel \tilde{k} and time slot \tilde{q} , it first demodulates the data packet to retrieve \mathbf{B}_{addr} and \mathbf{B}_{pcnt} from the packet header. Then, the GW converts them into decimal numbers D_{addr} and D_{pcnt} , respectively. It calculates the received code \tilde{X} as

$$\tilde{X} = \left(\tilde{k} - \sum_{k=0}^{\tilde{k}} (1 - a_k) \right) Q + \tilde{q}. \quad (6)$$

Then, transmission code \tilde{D}_{plim} is obtained by

$$\tilde{D}_{\text{plim}} = \text{mod} \left(\tilde{X} - f(D_{\text{addr}}, D_{\text{pcnt}}), R \right). \quad (7)$$

In (7), divisor $\tilde{X} - f(D_{\text{addr}}, D_{\text{pcnt}})$ may take a negative value, but \tilde{D}_{plim} always takes a positive value because the modulo operation is defined by (4). Finally, \tilde{D}_{plim} is converted into binary number to obtain $\tilde{\mathbf{B}}_{\text{plim}}$.

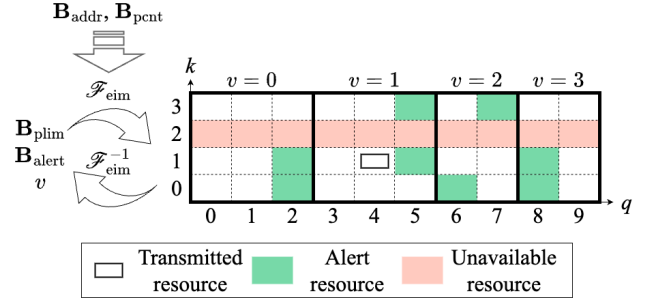


Fig. 1. Enhanced index mapper and de-mapper.

C. PLIM Issues

PLIM and flexible index mapping select one frequency channel k and one time slot q from R available resources according to the PLIM bit sequence \mathbf{B}_{plim} . If the transmission of another EN is detected by CAD or CS before transmission on the transmission resource (k, q) , the packet is discarded. In other words, each packet is given only one chance to be transmitted; if it cannot be transmitted in that chance, the payload bit is discarded in addition to the PLIM bit, which may reduce transmission efficiency.

III. ENHANCED INDEX MAPPER AND DE-MAPPER

A. Overview

This paper proposes an enhanced index mapper and de-mapper that takes into account frame division and alert transmission, as shown in Fig. 1. Taking advantage of the excessive resources in PLIM, the enhanced index mapper can transmit information called “alert” instead of PLIM bit sequence. Each node divides its frame into V_d subframes according to the predetermined criterion.¹ In the enhanced index mapper, the PLIM bit sequence \mathbf{B}_{plim} or the alert bit sequence $\mathbf{B}_{\text{alert}}$ is represented using resources in subframe v ($0 \leq v < V_d$). When the EN transmits the PLIM bit sequence \mathbf{B}_{plim} , it is mapped to a resource in input subframe v , excluding the unavailable frequency channels and the alert resources. Further, when the EN transmits an alert bit sequence $\mathbf{B}_{\text{alert}}$, it is mapped to an alert resource in input subframe v . The enhanced index mapper \mathcal{F}_{eim} takes transmit PLIM bit sequence \mathbf{B}_{plim} , transmit alert bit sequence $\mathbf{B}_{\text{alert}}$, and transmit subframe v as arguments; it is expressed as

$$(k, q) = \mathcal{F}_{\text{eim}}(\mathbf{B}_{\text{plim}}, \mathbf{B}_{\text{alert}}, v). \quad (8)$$

Index mapper \mathcal{F}_{eim} becomes a bijective function, any function can be used. The enhanced index de-mapper $\mathcal{F}_{\text{eim}}^{-1}$ returns received alert bit sequence $\tilde{\mathbf{B}}_{\text{alert}}$ and received subframe \tilde{v} , in addition to the PLIM bit sequence $\tilde{\mathbf{B}}_{\text{plim}}$; it is expressed as

$$(\tilde{\mathbf{B}}_{\text{plim}}, \tilde{\mathbf{B}}_{\text{alert}}, \tilde{v}) = \mathcal{F}_{\text{eim}}^{-1}(k, q). \quad (9)$$

Note that the enhanced index mapper \mathcal{F}_{eim} and de-mapper $\mathcal{F}_{\text{eim}}^{-1}$ use parameters such as device address \mathbf{B}_{addr} and packet counter \mathbf{B}_{pcnt} , in addition to the arguments in

¹Please note that this paper proposes a concept of EIM. Determining how to divide a frame into subframes depends on multiple factors such as system preferences, system size, hardware requirements, etc., which is beyond the scope of this paper.

equations (8) and (9). Relevant details are provided in Sections III-B and III-C.

Next, we explain the function of frame division. The R available resources are divided into V_d subframes, and the resources in each subframe are used to represent the PLIM bit sequence. The number of frame divisions V_d is expressed as an arbitrary function uniquely determined by frame division index d . The number of resources in the v -th subframe $R_{d,v}$ is expressed as

$$R_{d,v} = \begin{cases} \lceil Q/V_d \rceil \times K_a \triangleq R_d^+ & (0 \leq v < V'_d) \\ \lfloor Q/V_d \rfloor \times K_a \triangleq R_d^- & (V'_d \leq v < V_d), \end{cases} \quad (10)$$

where $V'_d = \text{mod}(Q, V_d)$ and the number of resources for each subframe can be set as in Eq. (10) to utilize all available resources. The number of PLIM bits of the proposed scheme B_{plim} can be expressed as $B_{\text{plim}} = \lfloor \log_2 R_d^- \rfloor$; hence, B_{plim} decreases as V_d increases.

Next, we describe the function of alert transmission. The enhanced index mapper can represent R_{alert} ($0 \leq R_{\text{alert}} < R$) types of alerts. Since this alert is a packet-level alert, it can be received even if the demodulation of the packet fails. Let us define the alert bit sequence as $\mathbf{B}_{\text{alert}}$ and its decimal representation as D_{alert} ($0 \leq D_{\text{alert}} \leq R_{\text{alert}}$). If $D_{\text{alert}} = 0$, no alert is defined. In particular, when $R_{\text{alert}} \leq R_{d,v} - 2^{\lfloor \log_2 R_{d,v} \rfloor}$, the alert bit sequence can be represented without reducing the number of PLIM bits B_{plim} . When an EN is configured to send an alert, information cannot always be transmitted in the PLIM bit sequence but can be transmitted in the payload bit sequence. Alert transmission can also be used for applications other than those assumed herein.

By setting $V_d = 1$ and $R_{\text{alert}} = 0$, the operation becomes similar to the conventional scheme [29], except for the resource counting direction. In [29], the counting direction of the index is always the time slot first, while that is always the frequency channel first in the proposed scheme. An arbitrary function, which is uniquely determined by the three variables $D_{\text{addr}}, D_{\text{pcent}}$, and v , can be used for the index mapper and de-mapper. The function $f(D_{\text{addr}}, D_{\text{pcent}}, v)$ is expressed as

$$\begin{cases} f(\cdot) \triangleq f(D_{\text{addr}}, D_{\text{pcent}}, v) \\ \tilde{f}(\cdot) \triangleq f(D_{\text{addr}}, D_{\text{pcent}}, \tilde{v}). \end{cases} \quad (11)$$

Note that the arbitrary function defined in (11) is one of the elements used in the enhanced index mapper and de-mapper, and is different from the index mapper $\mathcal{F}_{\text{eim}}(\mathbf{B}_{\text{plim}}, \mathbf{B}_{\text{alert}}, v)$ or de-mapper $\mathcal{F}_{\text{eim}}^{-1}(k, q)$.

B. Enhanced Index Mapper

The EN converts the PLIM bit sequence \mathbf{B}_{plim} , alert bit sequence $\mathbf{B}_{\text{alert}}$, device address \mathbf{B}_{addr} , and packet counter $\mathbf{B}_{\text{pcent}}$ to decimal numbers that are expressed as $D_{\text{plim}}, D_{\text{alert}}, D_{\text{addr}}$, and D_{pcent} , respectively. Then, the EN calculates transmission code X as

$$X = X_1 + \text{mod}(X_2 + X_3, R_{d,v}), \quad (12)$$

Algorithm 1 Enhanced Index Mapper \mathcal{F}_{eim}

Require: $\mathcal{K}, \mathcal{Q}, \mathcal{A}, f, V_d, d$ {Pre-shared between EN and GW}
Require: $\mathbf{B}_{\text{addr}}, \mathbf{B}_{\text{pcent}}$ {Obtained from LoRaWAN header [10]}
Require: $\mathbf{B}_{\text{plim}}, \mathbf{B}_{\text{alert}}, v$
Ensure: (k, q)

- 1: Convert $\mathbf{B}_{\text{addr}}, \mathbf{B}_{\text{pcent}}, \mathbf{B}_{\text{plim}}$, and $\mathbf{B}_{\text{alert}}$ into a decimal number $D_{\text{addr}}, D_{\text{pcent}}, D_{\text{plim}}$, and D_{alert} , respectively
- 2: Calculate V_d
- 3: Calculate X_1 by Eq. (13)
- 4: Calculate X_2 by Eq. (14)
- 5: Calculate X_3 by Eq. (15)
- 6: Calculate X by Eq. (12)
- 7: $k \leftarrow 0$
- 8: $s \leftarrow 0$
- 9: **while true do**
- 10: $s \leftarrow s + a_k$
- 11: **if** $s > \text{mod}(X, K_a)$ **then**
- 12: **break**
- 13: **end if**
- 14: $k \leftarrow k + 1$
- 15: **end while**
- 16: $q \leftarrow \lfloor X/K_a \rfloor$

where X_1, X_2 , and X_3 are expressed as

$$X_1 = \begin{cases} 0 & (v = 0) \\ \sum_{v'=0}^{v-1} R_{d,v'} & (v > 0), \end{cases} \quad (13)$$

$$X_2 = \begin{cases} f'(\cdot) & (D_{\text{alert}} < R_{\text{alert}}) \\ \text{mod}(f'(\cdot) + R_{\text{alert}}, R_{d,v}) & (D_{\text{alert}} = R_{\text{alert}}), \end{cases} \quad (14)$$

$$X_3 = \begin{cases} D_{\text{alert}} & (D_{\text{alert}} < R_{\text{alert}}) \\ \text{mod}(D_{\text{plim}} + f(\cdot), R_{d,v} - R_{\text{alert}}) & (D_{\text{alert}} = R_{\text{alert}}), \end{cases} \quad (15)$$

where $f'(\cdot) = \text{mod}(f(\cdot), R_{d,v})$ is an arbitrary function normalized by the number of the resources in the v -th subframe. Finally, the EN obtains transmission index (k, q) from X as

$$(k, q) = \left(\min \mathcal{K}', \left\lfloor \frac{X}{K_a} \right\rfloor \right), \quad (16)$$

where

$$\mathcal{K}' = \{k' \mid \text{mod}(X, K_a) + 1 = s_{k'} \in \mathcal{S}\} \subseteq \mathcal{K}, \quad (17)$$

and

$$\mathcal{S} = \{s_0, \dots, s_k, \dots, s_{K-1}\}, s_k = \sum_{k'=0}^k a_{k'}. \quad (18)$$

The mapping algorithm is shown in Algorithm 1.

C. Enhanced Index De-Mapper

The GW converts \mathbf{B}_{addr} and $\mathbf{B}_{\text{pcent}}$ into decimal numbers D_{addr} and D_{pcent} , respectively. Then, it calculates the received code Y as

$$Y = \left(\tilde{k} - \sum_{k=0}^{\tilde{k}} (1 - a_k) \right) + \tilde{q} \times K_a. \quad (19)$$

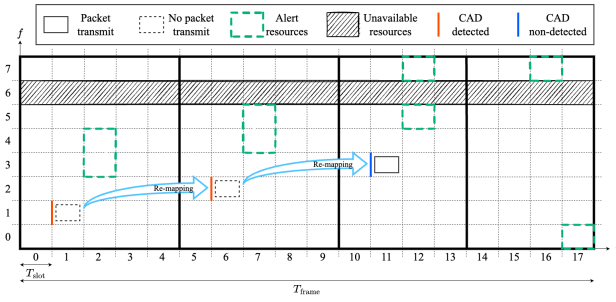


Fig. 2. CAD-based PLIM with enhanced index mapping.

It then calculates the received subframe \tilde{v} as

$$\tilde{v} = \begin{cases} \lfloor Y/R_d^+ \rfloor & (0 \leq Y < V_d' \times R_d^+) \\ V_d' + \lfloor Y/R_d^- \rfloor & (V_d' \times R_d^+ \leq Y < R). \end{cases} \quad (20)$$

And the subframe received code Y' is calculated as

$$Y' = \begin{cases} \text{mod}(Y, R_d^+) & (0 \leq \tilde{v} < V_d') \\ \text{mod}(Y - V_d' \times R_d^+, R_d^-) & (V_d' \leq \tilde{v} < V_d). \end{cases} \quad (21)$$

Then, the received PLIM bit sequence in decimal number \tilde{D}_{plim} and alert bit sequence in decimal number \tilde{D}_{alert} is obtained by

$$\tilde{D}_{\text{plim}} = \begin{cases} 0 & (Y' \in \mathcal{R}_{\text{alert}}) \\ Y' - \text{mod}(\tilde{f}'(\cdot) + R_{\text{alert}}, R_{d,\tilde{v}}) & (Y' \notin \mathcal{R}_{\text{alert}}), \end{cases} \quad (22)$$

$$\tilde{D}_{\text{alert}} = \begin{cases} \text{mod}(Y' - \tilde{f}'(\cdot)) & (Y' \in \mathcal{R}_{\text{alert}}) \\ 0 & (Y' \notin \mathcal{R}_{\text{alert}}), \end{cases} \quad (23)$$

where $\tilde{f}'(\cdot) = \text{mod}(\tilde{f}(\cdot), R_{d,\tilde{v}})$ is an estimated arbitrary function normalized by the number of the resources in the \tilde{v} -th subframe and $\mathcal{R}_{\text{alert}}$ is the set of the alert resources expressed as

$$\mathcal{R}_{\text{alert}} \triangleq \{ \text{mod}(f'(\cdot) + D_{\text{alert}}, R_{d,\tilde{v}}) \mid 0 \leq D_{\text{alert}} < R_{\text{alert}}, D_{\text{alert}} \in \mathbb{N}^+ \}. \quad (24)$$

Finally, \tilde{D}_{plim} and \tilde{D}_{alert} are converted into binary number to obtain $\tilde{\mathbf{B}}_{\text{plim}}$ and $\tilde{\mathbf{B}}_{\text{alert}}$, respectively. Note that upon receiving an alert, the de-mapper $\mathcal{F}_{\text{eim}}^{-1}$ returns $\tilde{\mathbf{B}}_{\text{plim}} = \mathbf{0}$; however, this sequence has no meaning and the zero vector is not sent as an information bit sequence. The de-mapping algorithm is shown in Algorithm 2.

IV. CAD-BASED PLIM

A. Overview

In this section, we describe a CAD-based PLIM scheme to improve throughput by flexibly dividing a frame into multiple subframes so that an EN can have multiple transmission opportunities for each packet. The proposed scheme consists of two main operations: (i) flexible determination of the number of frame divisions V_d and (ii) packet transmission using enhanced index mapper and CAD. Figure 2 shows a brief description of the CAD-based PLIM with enhanced index mapping.

Algorithm 2 Enhanced Index De-Mapper $\mathcal{F}_{\text{eim}}^{-1}$

Require: $\mathcal{K}, \mathcal{Q}, \mathcal{A}, f, V_d, d$ {Pre-shared between EN and GW}

Require: (k, \tilde{q}) {Obtained by the GW [26]}

Require: $\mathbf{B}_{\text{addr}}, \mathbf{B}_{\text{pcent}}$ {Obtained from packet header [10]}

Ensure: $\tilde{\mathbf{B}}_{\text{plim}}, \tilde{\mathbf{B}}_{\text{alert}}$

- 1: Convert \mathbf{B}_{addr} and $\mathbf{B}_{\text{pcent}}$ into binary number D_{addr} and D_{pcent} , respectively
- 2: $R_d^+ \leftarrow \lceil Q/V_d \rceil \times K_a$
- 3: $R_d^- \leftarrow \lfloor Q/V_d \rfloor \times K_a$
- 4: $V_d' \leftarrow \text{mod}(Q, V_d)$
- 5: Calculate Y by Eq. (19)
- 6: Calculate \tilde{v} by Eq. (20)
- 7: Calculate Y' by Eq. (21)
- 8: $\tilde{f}'(\cdot) \leftarrow \text{mod}(\tilde{f}(\cdot), R_{d,\tilde{v}})$
- 9: $M \leftarrow \text{mod}(f'(\cdot) + R_{\text{alert}}, R_{d,\tilde{v}})$
- 10: **if** $((0 < M < R_{\text{alert}}) \& (Y' < M \mid f'(\cdot) \leq Y')) \mid ((M = 0 \mid R_{\text{alert}} \leq M) \& (f'(\cdot) \leq Y' < M))$ **then**
- 11: $D_{\text{plim}} \leftarrow 0$
- 12: $D_{\text{alert}} \leftarrow \text{mod}(Y' - \tilde{f}'(\cdot))$
- 13: **else**
- 14: $D_{\text{plim}} \leftarrow Y' - \text{mod}(\tilde{f}'(\cdot) + R_{\text{alert}}, R_{d,\tilde{v}})$
- 15: $D_{\text{alert}} \leftarrow 0$
- 16: **end if**
- 17: Convert \tilde{D}_{plim} and \tilde{D}_{alert} into binary number $\tilde{\mathbf{B}}_{\text{plim}}$ and $\tilde{\mathbf{B}}_{\text{alert}}$, respectively

A larger V_d provides more transmission opportunities to an EN; hence, it may reduce the number of packets discarded. However, as V_d increases, the number of bits that PLIM can represent decreases. Thus, there is a trade-off between packet discard and throughput. Therefore, it is necessary to flexibly change V_d to reduce the packet discard rate while suppressing the decrease in the number of bits transmitted by PLIM. This paper proposes a scheme to flexibly determine V_d based on the number of consecutive successful and failed packet transmissions. Here, a successful transmission is considered when an EN sends a UNC packet or sends a CONF packet and receives an ACK packet; further, a transmission failure is considered when an EN discards a packet or sends a CONF packet but receives no ACK packet.

Let d denote the frame division index, which is initialized to d_{init} and varies within a range of $d_{\text{min}} \leq d \leq d_{\text{max}}$, where d_{min} is the minimum frame division index and d_{max} is the maximum frame division index. When the number of consecutive transmission failure frames j exceeds the division threshold j_{th} , an EN sends a CONF packet with the mapped resource as $D_{\text{alert}} = 2$ and divides the frame after receiving an ACK packet from the GW (increment d). When the number of consecutive transmission successful frames i exceeds the concatenation threshold i_{th} , the EN sends a CONF packet with the resource mapped as $D_{\text{alert}} = 1$ and concatenates subframes after receiving an ACK packet from the GW (decrement d).

An EN selects a transmission resource within the 0th subframe and performs CAD at the start of the selected transmission resource. Specifically, the EN calculates the cross-correlation between the internally generated LoRa signal and the received LoRa signal, and compares it with a threshold value to detect signals from other ENs. It then transmits the packet if CAD does not detect ongoing transmission. However, if CAD detects ongoing transmission, the EN does

not transmit the packet in the selected transmission resource. Instead, it selects another resource in the subsequent subframe and performs CAD again. If the EN cannot transmit the packet, it repeats this operation for the rest of the subframes. If the EN cannot transmit the packet by the end of the frame, that is, V_d consecutive CAD detections, the EN discards the information bit sequence. In other words, the EN gets V_d opportunities to transmit a packet. Note that it is also possible to use CS instead of CAD.

B. Algorithm for EN

Without loss of generality, we now focus on one specific EN to explain the operation of the proposed scheme. Notably, the proposed scheme does not require any synchronization between ENs.

An EN initializes various parameters used for mapping and waits until an information bit sequence is generated. Once generated, the EN performs a frame division/concatenation decision based on d , i , and j . For frame division, the EN sets the alert bit sequence to $D_{\text{alert}} = 0$; however, in the case of frame concatenation, the EN sets the alert bit sequence to $D_{\text{alert}} = 1$. Then, it determines the transmit frequency channel k and the time slot q by enhanced index mapper \mathcal{F}_{eim} and performs CAD at the beginning of time slot q on frequency channel k .

If CAD detects ongoing transmission on frequency channel k , the EN performs mapping in the subsequent subframe unless no subframe remains. If no subframe remains, it discards the generated packet. If CAD does not detect ongoing transmission, the packet is transmitted. If the EN performs either frame division or concatenation, it sends a CONF packet; otherwise, it sends a UNC packet. The details of the algorithm for an EN are shown in Fig. 3. In Fig. 3, $\text{rand}(m, n)$ returns a pseudorandom scalar integer between m and n .

C. Algorithm for GW

The GW initializes various parameters used for de-mapping for each EN and waits for an incoming data packet. When it receives a data packet on frequency channel \tilde{k} and time slot \tilde{q} , it demodulates the packet and retrieves \mathbf{B}_{addr} and $\mathbf{B}_{\text{pcent}}$. When a packet is received for the first time from the EN with device address \mathbf{B}_{addr} , \mathbf{B}_{addr} is stored in the GW memory as $d(\mathbf{B}_{\text{addr}}) = d_{\text{init}}$; when \mathbf{B}_{addr} has already been received, $d(\mathbf{B}_{\text{addr}})$ is called from the memory in the GW. Then, the GW obtains the PLIM bit sequence $\hat{\mathbf{B}}_{\text{plim}}$ using the de-mapping function $\mathcal{F}_{\text{eim}}^{-1}$. Finally, if a CONF packet is received, the GW updates $d(\mathbf{B}_{\text{addr}})$ according to the value of $\hat{\mathbf{B}}_{\text{plim}}$ and discards $\hat{\mathbf{B}}_{\text{plim}}$. Note that $\hat{\mathbf{B}}_{\text{plim}}$ in the CONF packet is not an information bit sequence generated by an EN; thus, $\hat{\mathbf{B}}_{\text{plim}}$ is discarded after d is updated. The details of the algorithm for GW are shown in Fig. 4.

V. PERFORMANCE EVALUATION

A. System Model

This section describes the performance evaluation of the proposed enhanced index mapper (EIM) and CAD-based

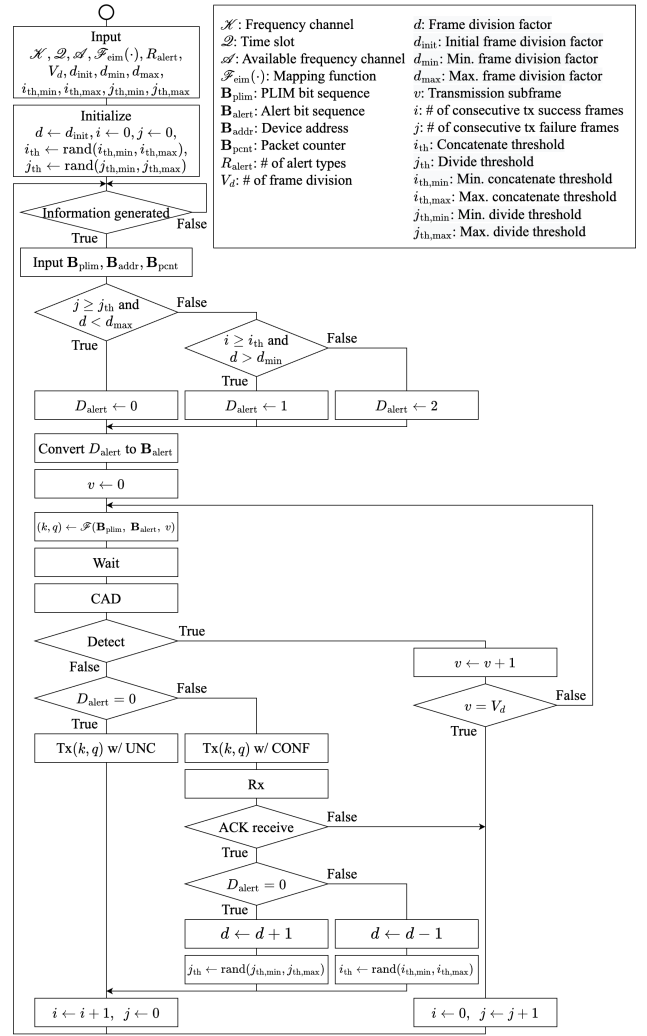


Fig. 3. Algorithm for EN.

PLIM through computer simulations conducted in the study. Table I shows the simulation parameters. Unless otherwise noted, the parameters listed in Table I were used for the evaluation.

We assumed a LoRaWAN system with N ENs randomly placed in a circular communication area of radius $r = 500$ [m] centered at the GW. Each EN was assumed to be asynchronous and generate a random transmit bit sequence with a fixed transmission period $T_{\text{frame}} = 180$ [sec]. The DC of ENs and the GW were assumed to be 1 % [31]. An EN transmits a packet with payload size $B_{\text{pl}} = 5$ [byte], overhead size $OH = 20.25$ [symbol], spreading factor $SF = 10$, coding rate $CR = 4/7$, carrier frequency $CF = \{922.0, 922.2, \dots, 923.2, 923.4\}$ [MHz], bandwidth $BW = 125$ [kHz], and transmit power $P_{\text{tx}} = 13$ [dBm] [31]. When the GW receives a CONF packet, it sends an ACK packet whose payload size $B_{\text{pl}} = 0$ [byte] as long as it can satisfy the DC constraint. We assumed that the EN can ideally receive the ACK packet if the GW sends it.

The propagation path model follows [30]. The received power of the signal transmitted from EN n at the GW, $P_{\text{rx}, n}$, is expressed as

$$P_{\text{rx}, n} = P_{\text{tx}} - (10\alpha \log_{10} l_n + \beta + 10\gamma \log_{10} CF) - \zeta, \quad (25)$$

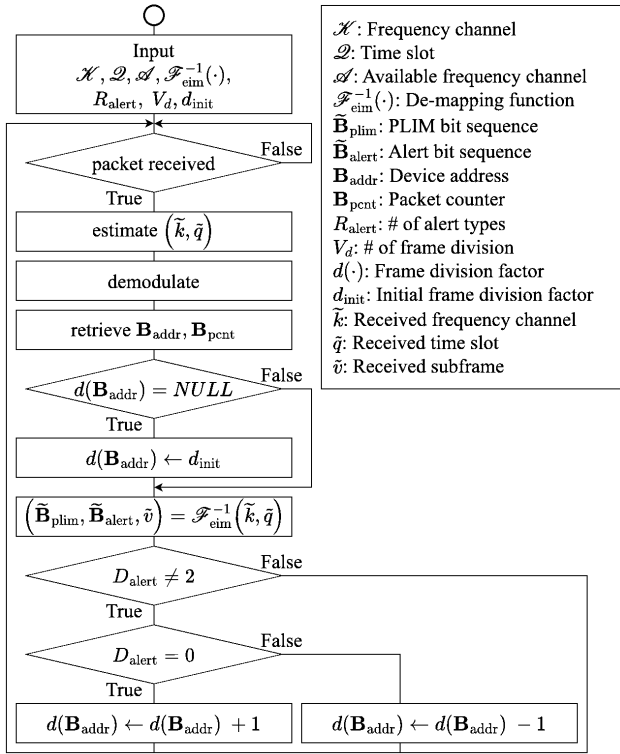


Fig. 4. Algorithm for GW.

where l_n [m] is the distance between the GW and EN n , α is the propagation coefficient, β is the propagation loss offset, γ is the frequency coefficient, and ζ is a random variable following a gaussian distribution with mean μ and variance σ . The signal-to-noise ratio (SNR) and the signal-to-interference ratio (SIR) of EN n observed at the GW are given by

$$\begin{cases} \gamma_{\text{snr},n} = P_{\text{rx},n} - (N_0 + 10\log_{10}BW + NF) \\ \gamma_{\text{sir},n} = P_{\text{rx},n} - \sum_{n' \in \mathcal{I}_n} P_{\text{rx},n'} \end{cases} \quad (26)$$

where N_0 [dBm/Hz] is the noise power spectrum density, NF is the noise figure, and \mathcal{I}_n is the set of interfering ENs that transmit packets using the same frequency channel as the EN n . The conditions for successful packet transmission are either the GW receiving a packet from one EN with the received SNR being larger than the threshold value Γ_{snr} or receiving multiple packets with one of them having the received SNR and SIR being larger than the threshold values Γ_{snr} and Γ_{sir} , respectively. Each EN performs CAD for $T_{\text{cad}} = (2^{SF} + 32)/BW$ [sec] [14] and determines whether there is ongoing transmission if the received SNR exceeds threshold value Γ_{snr} .

We assumed that the number of frame divisions is $V(d) = 2^d$ and the arbitrary function $f(D_{\text{addr}}, D_{\text{pcnt}}, v) = D_{\text{addr}} + D_{\text{pcnt}} + v$.

This section is organized as follows. Section V-B describes the evaluation of the effectiveness of the enhanced index mapper and de-mapper, while Section V-C discusses the same for CAD-based PLIM.

TABLE I
EVALUATION PARAMETERS

Parameter	Value
Area radius, r	500 [m]
Number of ENs, N	500
Number of frequency channels, K	8
Number of available frequency channels, K_a	5
Number of time slots, Q	300
Frame length, T_{frame}	120 [sec]
Duty cycle, DC	0.01
Payload size, B_{pl}	5 [byte]
Overhead size, OH	20.25 [symbol]
Spreading factor, SF	10
Coding rate, CR	4/7
Carrier frequency, CF	{922.0, 922.2, ..., 923.2, 923.4} [MHz]
Bandwidth, BW	125 [kHz]
Transmit power, P_{tx}	13 [dBm]
Propagation coefficient, α	4.0
Propagation loss offset, β	9.5
Frequency coefficient, γ	4.5
Mean of gaussian distribution, μ	0
Variance of gaussian distribution, σ	3.48 [dB]
Noise power spectrum density, N_0	-174 [dBm/Hz]
Noise figure, NF	10 [dB]
SNR threshold, Γ_{snr} [14]	-15 [dB]
SIR threshold, Γ_{sir} [13]	6 [dB]
Initial frame division exponents, d_{init}	3
Min. frame division exponents, d_{min}	0
Max. frame division exponents, d_{max}	6
Min. frame division threshold, $j_{\text{th},\text{min}}$	3
Max. frame division threshold, $j_{\text{th},\text{max}}$	4
Min. frame concatenation threshold, $i_{\text{th},\text{min}}$	5
Max. frame concatenation threshold, $i_{\text{th},\text{max}}$	8

B. Performance of Enhanced Index Mapper and De-Mapper

The distribution of the selected transmission resources was evaluated using Monte Carlo simulation with the number of frequency channels $K = 8$ and available frequency channels $\mathcal{A} = \{1, 1, 1, 0, 0, 0, 1, 1\}$, that is, frequency channels $k = 3, 4$, and 5 are not available. We considered the scenario when the number of available resources is $K_a = 5$ and the number of time slots is $Q = 300$. The values of device address B_{addr} and packet counter B_{pcnt} were set to be random. In EIM, the number of frame divisions and the number of alert resources were set to $V_d = \{4, 16\}$ and $R_{\text{alert}} = 2$, respectively, and subframe v was randomly selected from $0 \leq v < V_d$. When $V_d = 4$, the time slots can be divided equally, so the number of resources $R_{d,v} = 375$ for all subframes. However, when $V_d = 16$, the time slots cannot be equally divided, and $R_{d,v} = 95$ ($0 \leq v < 12$), 90 ($12 \leq v < 16$). The resource number w is uniquely determined by the frequency channel k , and the time slot q is defined as $w = k \times Q + q$.

In this section, the performance of the enhanced index mapper is labeled as ‘‘EIM’’, the flexible index mapping scheme [29] is labeled as ‘‘FIM’’,² the PLIM [26] is labeled as ‘‘PLIM’’.

1) *Resource Usage for PLIM Bit Sequence Transmission:* Figure 5 shows the probability mass function (PMF) of selecting transmission resource w , frequency channel k , and time slot q when random PLIM bit sequences are transmitted. Since

²The index mapper used in this paper has been slightly modified from [29] to accommodate arbitrary multiple unavailable frequency channels. Details are omitted for reasons of space.

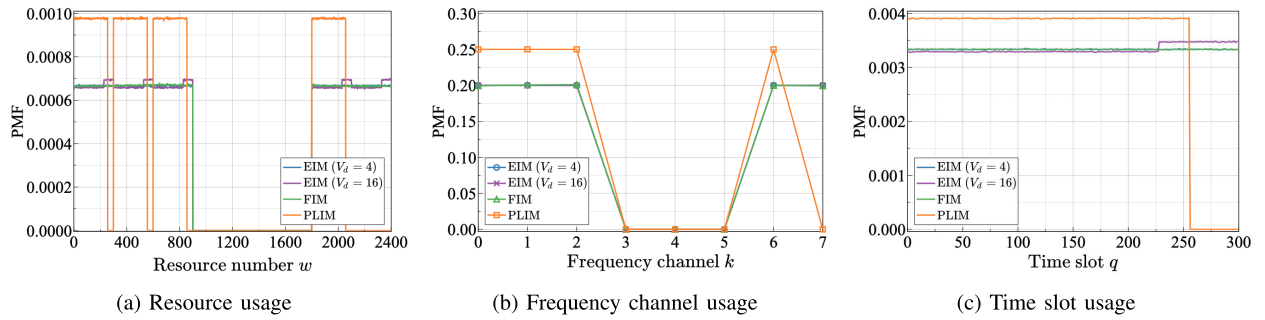


Fig. 5. Resource usage in PLIM bit sequence transmission.

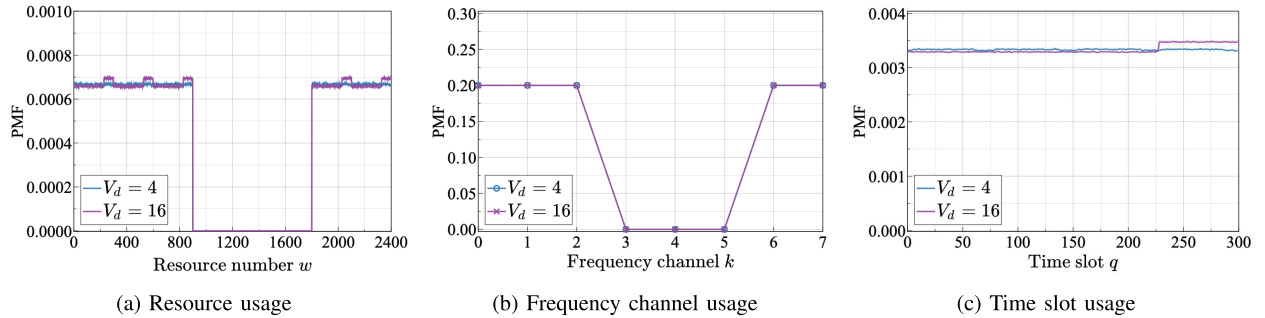


Fig. 6. Resource usage in alert bit sequence transmission.

PLIM directly allocates PLIM bit sequences to frequency channels and time slots, the number of frequency channels K and time slots Q are constrained to be $\log_2 K \in \mathbb{N}^+$ and $\log_2 Q \in \mathbb{N}^+$, respectively [26]. Thus, excess resources ($K \times Q - 2^{\lceil \log_2 K \rceil + \lceil \log_2 Q \rceil}$) cannot be selected in PLIM. FIM overcomes the above PLIM constraint; thus, all available resources except for the unavailable frequency channels can be approximately uniformly selected [29]. In EIM, when $V_d = 4$, all available resources except for the unavailable frequency channels are selected approximately uniformly like FIM. On the contrary, when $V_d = 16$, transmission resources are not selected uniformly. For example, resources with $0 \leq w < 228$ are selected less frequently than those with $228 \leq w < 300$. This is because the number of resources in subframes $0 \leq v < 12$ is larger than that for subframes $12 \leq v < 16$. When subframe v is selected uniformly, the larger the number of resources in a subframe, the smaller the percentage of each resource selected. However, each frequency channel is selected uniformly regardless of the value of V_d .

2) *Resource Usage for Alert Bit Sequence Transmission*: The proposed EIM exclusively allocates R_{alert} resources to the alert resources in each subframe. In other words, $V_d \times R_{\text{alert}}$ resources are allocated for alert transmission within a frame and these resources are not used for PLIM bit transmission. Suppose that alert resources are allocated unevenly to a particular frequency channel. In such a case, the frequency channel will be used less frequently for PLIM bit transmission, which may increase the number of packet collisions. Therefore, alert resources should be allocated uniformly for all frequency channels and time slots.

Figure 6 shows the PMF of the resources selected as alert resources in EIM. When $V_d = 4$, the alert resources are selected uniformly according to device address B_{addr} , packet counter B_{pcnt} , and subframe v . On the contrary,

when $V_d = 16$, resources are not selected uniformly as alert resources. This is because the number of resources in each subframe is not equal, as in the case of PLIM bit transmission. However, the frequency channel is selected uniformly regardless of the value of V_d .

C. Performance of CAD-Based PLIM

This subsection describes the performance evaluation of the CAD-based PLIM. Section V-C.1 discusses the performance evaluation when all ENs use a fixed same number of frame divisions. In Section V-C.2, V-C.3, and V-C.4, we respectively describe the evaluation of the number of ENs, the number of available frequency channels, and distance performance when the number of frame divisions for each EN is adaptively varied using CAD-based PLIM. Section V-C.5 describes the evaluation of the fairness of each EN. Section V-C.6 describes the evaluation of the computational complexity for the proposed scheme and the conventional scheme. Hereinafter, the performance of the CAD-based PLIM is labeled as ‘‘Proposed’’, the flexible index mapping scheme [29] with CAD is labeled as ‘‘FIM w/ CAD’’, the flexible index mapping scheme [29] is labeled as ‘‘FIM’’, the PLIM [26] is labeled as ‘‘PLIM’’, and the conventional LoRaWAN transmission as ‘‘ALOHA’’, respectively. In ‘‘FIM w/ CAD’’, an EN performs CAD before sending a packet and discards the packet if it detects another EN’s signal. In other words, ‘‘FIM w/ CAD’’ is a scheme that adds LBT and pseudorandom backoff to FIM.

1) *Effects of Number of Subframes*: In EIM, dividing a frame into V_d subframes provides V_d opportunities to send packets. As the number of frame divisions V_d increases, the transmission opportunities increase but the number of PLIM bits B_{plim} decreases. Thus, there is a trade-off between transmission opportunities and the number of PLIM bits. Herein, the impact of V_d on the system performance was evaluated;

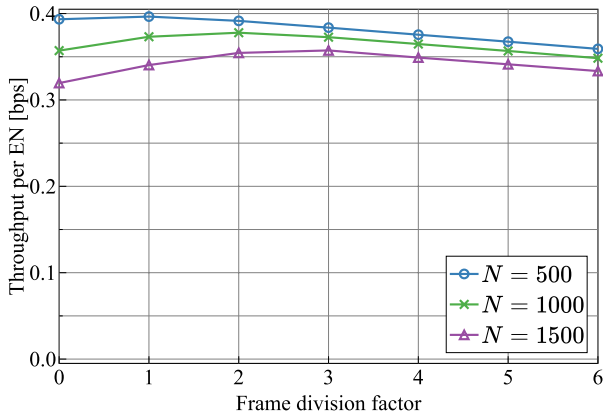


Fig. 7. Throughput vs frame division factor.

specifically, throughput, the ratio of packet transmission success, failure, discard, and average latency. It was assumed that all ENs are set to the same number of divisions V_d . In other words, the initial frame division exponents d_{init} , minimum frame division exponents d_{min} , and maximum frame division exponents d_{max} were set to the same value.

Average throughput per EN S [bps] is defined as

$$S = D_{\text{rx}} / (N \times T_{\text{sim}}), \quad (27)$$

where D_{rx} [bit] is the total received data size at the GW, N is the number of ENs, and T_{sim} [sec] is the simulation time. Figure 7 shows the average throughput per EN S [bps] versus frame division factor d . The figure shows that throughput S is maximized at $d = 1$ ($N = 500$), 2 ($N = 1000$), 3 ($N = 1500$), respectively, and decreases beyond those values. In other words, there is an optimum number of frame divisions that maximizes throughput (denoted as d^*) depending on the value of N . This indicates that when d is greater than d^* , the impact of the decrease in the number of PLIM bits is more dominant than the increase in transmission opportunities.

To examine the reasons for the decrease in throughput, the ratio of packet transmission success, failure, and discard were evaluated. All packets are either transmitted or discarded. If a packet is transmitted, its reception at the GW is either success or failure. In other words, $P_s + P_f + P_d = 1$, where P_s , P_f , and P_d represent the ratios of transmission success, failure, and discard, respectively. Figure 8 shows P_s , P_f , and P_d versus frame division factor d . Depending on the value of N , there exists a d that maximizes P_s . On the contrary, regardless of the value of N , as d increases, P_f increases and P_d decreases. Since P_s , P_f , P_d , and the number of PLIM bits B increase or decrease with the value of d , the value of d^* varies with N .

The normalized average latency L is defined as

$$L = (T_{\text{rx}} - T_{\text{tx}}) / T_{\text{frame}}, \quad (28)$$

where T_{rx} [sec] is the packet received time at the GW and T_{tx} [sec] is the packet generation time at the EN. Figure 9 shows normalized average latency L versus frame division factor d . As d increases, the probability of selecting the resources in the earlier subframe becomes higher, resulting in smaller latency. To reduce the latency, the frame division factor d should be increased.

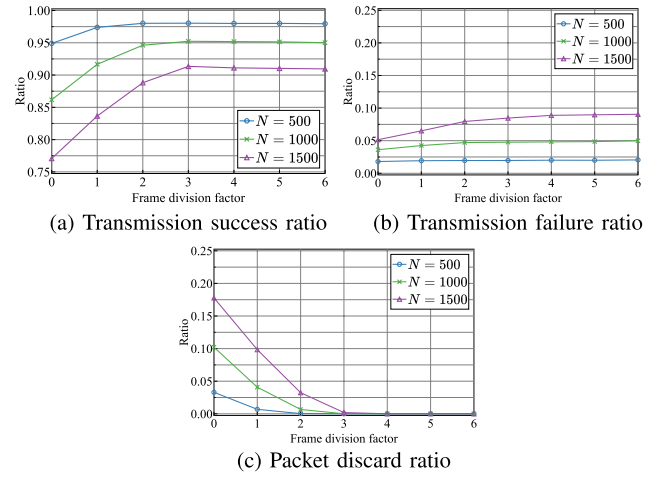


Fig. 8. Ratio of packet transmission success, failure, and discard vs frame division factor.

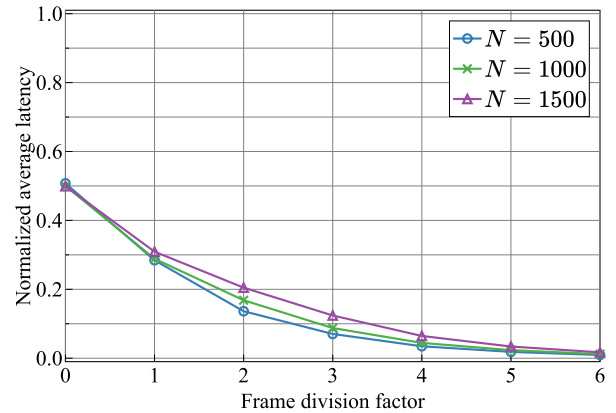


Fig. 9. Normalized average latency vs frame division factor.

2) *Effects of Number of ENs*: Figure 10 shows throughput S [bps] versus number of ENs N . Due to the information-bearing index, PLIM transmission can improve the throughput performance compared to conventional LoRaWAN (ALOHA). FIM can further improve the throughput performance due to the following two factors. The first factor is reduced packet collisions due to the mapping of the information-bearing index to all the available frequency channels and time slots. The second factor is the increased number of information bits conveyed by the index by jointly assigning the index to frequency channels and time slots. The proposed scheme further improves throughput and closes to the upperbound³ compared to FIM [29] regardless of the SF values. In particular, it increases by a factor of 1.20 with $N = 1000$ and $SF = 10$. The factor that contributes to the increased throughput is discussed below.

Figure 11 shows P_s , P_f , and P_d as a function of number of ENs N . The proposed scheme increases P_s and decreases P_d compared to FIM [29] due to the increased transmission opportunities by adaptive frame division. The proposed scheme also increases P_f by failed CAD and sending packets while other

³The throughput upperbound of PLIM is achieved when all the time and frequency channels are used for the index. The particular upperbound becomes $(B_{\text{pl}} + B_{\text{plim}}) / T_{\text{frame}} = 0.417$ [bps] in the simulation setup. If there is no packet collision between ENs, this upperbound can be obtained for all the ENs.

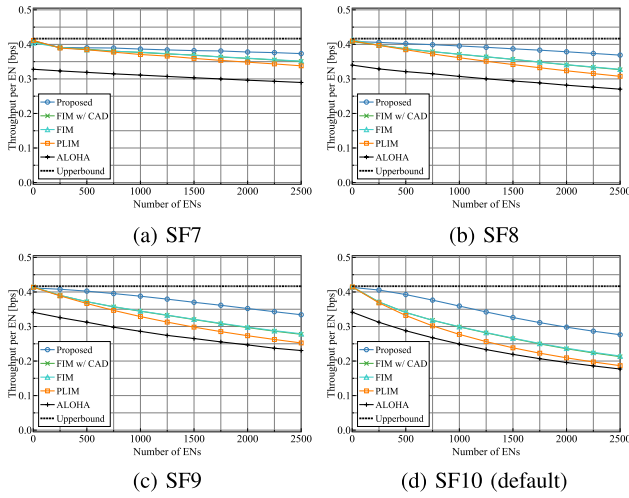


Fig. 10. Throughput vs number of ENs.

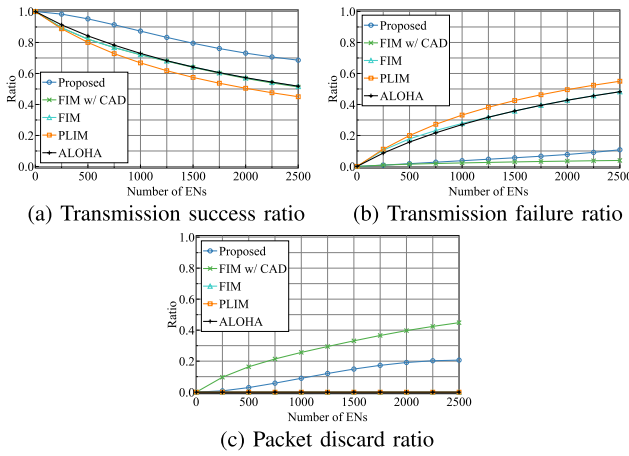


Fig. 11. Ratio of packet transmission success, failure, and discard vs number of ENs.

ENs are sending packets. However, the throughput increases because the impact of the decreased P_d is dominant.

3) *Effect of Number of Available Channels:* Figure 12 shows throughput S [bps] as a function of number of available frequency channels K_a . The proposed scheme improves the throughput compared to conventional schemes. This is due to the adaptive frame division, as discussed in Section V-C.2. In particular, the throughput improves approximately 1.15 times when $K_a = 5$. When K_a is a power of 2, the throughput performance of “FIM” and “PLIM” is almost the same because “PLIM” can use all available frequency channels. On the contrary, the proposed scheme significantly improves throughput regardless of K_a .

4) *Effects of Area Size:* Figure 13 shows the throughput S [bps] versus the area radius r [m]. The proposed scheme can increase the throughput compared to FIM irrespective of area radius r . When the area radius is greater than 1000 [m], the improvement in throughput for the proposed scheme becomes smaller. This is because when the area radius is larger than 1000 [m], many ENs cannot detect the signals of other ENs with CAD. In other words, the performance of the proposed scheme and FIM are almost equal in situations where CAD does not work effectively. The proposed scheme works effectively for systems with a radius of less than 1000 [m].

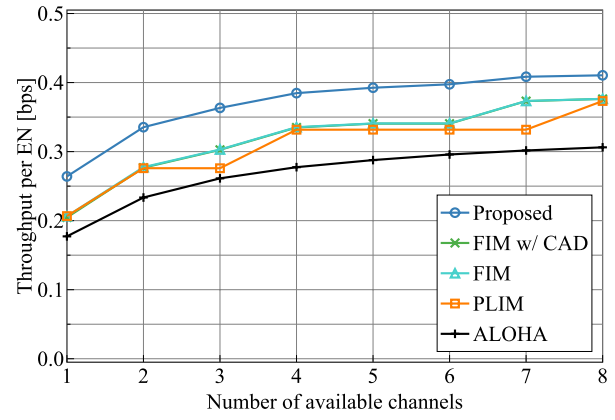


Fig. 12. Throughput vs number of available channels.

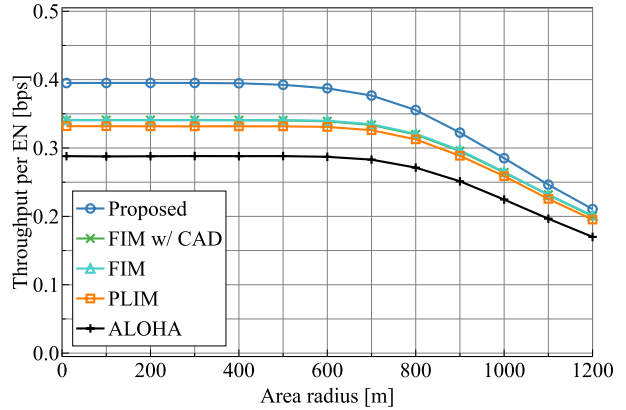


Fig. 13. Throughput vs area radius.

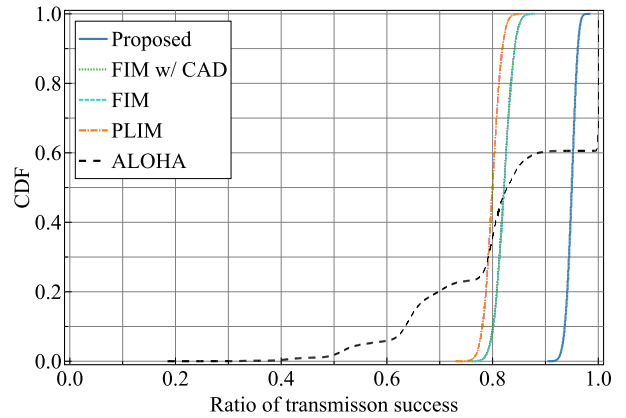


Fig. 14. CDF of the packet transmission success ratio.

5) *Fairness:* Next, the cumulative distribution functions (CDFs) of packet transmission success ratio P_s and normalized average latency L were evaluated.

Figure 14 shows the CDF of the packet transmission success ratio P_s .⁴ The proposed scheme improves P_s for all ENs compared to the conventional schemes. This is due to the adaptive frame division, as discussed in Section V-C.2.

⁴When ALOHA was used in the system model in this study, the packet collision ratio of each EN was determined by the number of ENs whose first packet transmission durations overlap and packets continue to collide at that packet collision ratio from the second packet onward, so they are distributed around some packet transmission success ratio. An in-depth discussion of ALOHA’s performance is beyond the scope of this study.

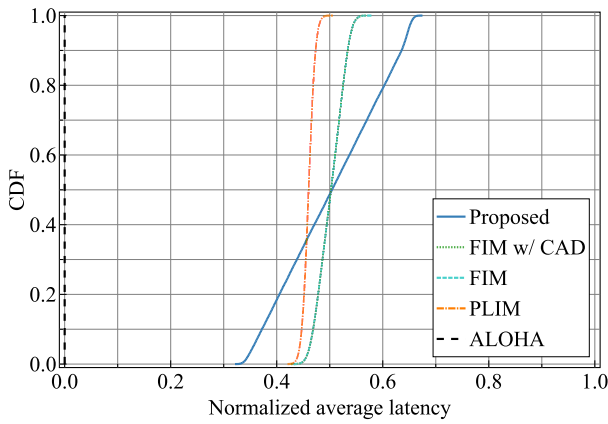


Fig. 15. CDF of the normalized average latency.

Figure 15 shows the CDF of normalized average latency L . The average latency of the proposed scheme is equal to that of the conventional scheme, but the variance is larger. In other words, the proposed scheme increases the number of low-latency ENs and high-latency ENs. The proposed scheme improves throughput by distributing the transmission timing of each EN over the entire frame.

6) *Complexity*: Finally, time complexity, one of the computational complexity metrics, is calculated for the conventional and proposed schemes. In the conventional scheme, an EN determines frequency channel k and time slot q in a fixed number of steps for each packet transmission, whose complexity can be expressed as $O(1)$. On the other hand, in the proposed scheme, an EN calculates frequency channel k and time slot q at most $2^{d_{\max}}$ times before transmitting a data packet. Thus, its complexity can be expressed as $O(2^{d_{\max}})$ where d_{\max} is the maximum frame division exponents that can be arbitrarily selected within the range of $0 \leq d_{\max} \leq \lfloor \log_2 Q \rfloor$. In a typical application scenario, as in the manuscript, each EN transmits one data packet every minute to a few hours. In such a scenario, we have $10^1 < Q < 10^5$. Furthermore, from the viewpoint of practicability and effectiveness, the number of frame division $2^{d_{\max}}$ is at most up to a few hundred, and hence the complexity at the EN is not high. In simulation results, we have set $d_{\max} = 6$ and it has been shown that the proposed method can provide significant performance gain. The GW calculates PLIM bit sequence \mathbf{B}_{plim} in a fixed number of steps in both the conventional and proposed schemes. Therefore, the complexity of the GW can be expressed as $O(1)$ regardless of the scheme.

VI. CONCLUSION

This study developed an index mapping scheme using adaptive frame division and CAD to improve the throughput performance of packet-level index modulation (PLIM). The proposed scheme divides a transmission frame into multiple subframes and performs CAD before transmission in each subframe to increase the chances of packet transmission and reduce the packet discard rate. The proposed scheme benefits from the improvement in the amount of data transmitted by PLIM even when the number of available channels and end nodes changes. Computer simulation evaluations showed that the proposed scheme improves throughput performance by

approximately 20% compared to the conventional scheme. Future work would include the evaluation of the proposed scheme through experiments on actual equipment.

REFERENCES

- [1] A. Al-Fuqaha, M. Guizani, M. Mohammadi, M. Aledhari, and M. Ayyash, "Internet of Things: A survey on enabling technologies, protocols, and applications," *IEEE Commun. Surveys Tuts.*, vol. 17, no. 4, pp. 2347–2376, 4th Quart., 2015.
- [2] A. Whitmore, A. Agarwal, and L. Da Xu, "The Internet of Things—A survey of topics and trends," *Inf. Syst. Frontiers*, vol. 17, no. 2, pp. 261–274, Apr. 2015.
- [3] L. Atzori, I. A. Iera, and M. Giacomo, "The Internet of Things: A survey," *Comput. Netw.*, vol. 54, pp. 2787–2805, May 2010.
- [4] L. D. Xu, W. He, and S. Li, "Internet of Things in industries: A survey," *IEEE Trans. Ind. Informat.*, vol. 10, no. 4, pp. 2233–2243, Nov. 2014.
- [5] J. Ko, C. Lu, M. B. Srivastava, J. A. Stankovic, A. Terzis, and M. Welsh, "Wireless sensor networks for healthcare," *Proc. IEEE*, vol. 98, no. 11, pp. 1947–1960, Nov. 2010.
- [6] H. Wang and A. O. Fapojuwo, "A survey of enabling technologies of low power and long range machine-to-machine communications," *IEEE Commun. Surveys Tuts.*, vol. 19, no. 4, pp. 2621–2639, 4th Quart., 2017.
- [7] A. Lavric and V. Popa, "Internet of Things and LoRa low-power wide-area networks: A survey," in *Proc. Int. Symp. Signals, Circuits Syst. (ISSCS)*, Jul. 2017, pp. 1–5.
- [8] K. Mekki, E. Bajic, F. Chaxel, and F. Meyer, "A comparative study of LPWAN technologies for large-scale IoT deployment," *ICT Exp.*, vol. 5, no. 1, pp. 1–7, Mar. 2019.
- [9] U. Raza, P. Kulkarni, and M. Sooriyabandara, "Low power wide area networks: An overview," *IEEE Commun. Surveys Tuts.*, vol. 19, no. 2, pp. 855–873, 2nd Quart., 2017.
- [10] *LoRaWAN® L2 1.0.4 Specification*, Standard TS001-1.0.4, Oct. 2020.
- [11] J. P. Shanmuga Sundaram, W. Du, and Z. Zhao, "A survey on LoRa networking: Research problems, current solutions, and open issues," *IEEE Commun. Surveys Tuts.*, vol. 22, no. 1, pp. 371–388, 1st Quart., 2020.
- [12] *LoRaWAN® Regional Parameters*, document RP002-1.0.4, Sep. 2022.
- [13] O. Georgiou and U. Raza, "Low power wide area network analysis: Can LoRa scale?" *IEEE Wireless Commun. Lett.*, vol. 6, no. 2, pp. 162–165, Apr. 2017.
- [14] *SX1276/77/78/79—137 MHz to 1020 MHz Low Power Long Range Transceiver*, Rev. 7, Semtech, Camarillo, CA, USA, May 2020.
- [15] A. Gamage, J. C. Liando, C. Gu, R. Tan, and M. Li, "LMAC: Efficient carrier-sense multiple access for LoRa," in *Proc. 26th Annu. Int. Conf. Mobile Comput. Netw.*, no. 43, Apr. 2020, pp. 1–13.
- [16] M. O'Kennedy, T. Niesler, R. Wolhuter, and N. Mitton, "Practical evaluation of carrier sensing for a LoRa wildlife monitoring network," in *Proc. IFIP Netw. Conf. (Networking)*, Jun. 2020, pp. 614–618.
- [17] C. Pham, "Investigating and experimenting CSMA channel access mechanisms for LoRa IoT networks," in *Proc. IEEE Wireless Commun. Netw. Conf. (WCNC)*, Apr. 2018, pp. 1–6.
- [18] T.-H. To and A. Duda, "Simulation of LoRa in NS-3: Improving LoRa performance with CSMA," in *Proc. IEEE Int. Conf. Commun. (ICC)*, May 2018, pp. 1–7.
- [19] J. Ortín, M. Cesana, and A. Redondi, "Augmenting LoRaWAN performance with listen before talk," *IEEE Trans. Wireless Commun.*, vol. 18, no. 6, pp. 3113–3128, Jun. 2019.
- [20] M. H. Tsoi, T. H. Ng, D. P. K. Lun, Y. S. Choy, and S. W. Y. Mung, "LoRa data throughput enhancement by slotted channel activity detection," in *Proc. IEEE Asia-Pacific Microw. Conf. (APMC)*, Dec. 2020, pp. 466–468.
- [21] E. M. Rochester, A. M. Yousuf, B. Ousat, and M. Ghaderi, "Lightweight carrier sensing in LoRa: Implementation and performance evaluation," in *Proc. IEEE Int. Conf. Commun. (ICC)*, Jun. 2020, pp. 1–6.
- [22] K. Kamonkusonman and R. Silapunt, "Channel activity detection with the modified backoff algorithm for LoRaWAN," in *Proc. 18th Int. Conf. Electr. Eng./Electron., Comput., Telecommun. Inf. Technol. (ECTI-CON)*, May 2021, pp. 86–89.
- [23] L. Beltramelli, A. Mahmood, P. Österberg, and M. Gidlund, "LoRa beyond ALOHA: An investigation of alternative random access protocols," *IEEE Trans. Ind. Informat.*, vol. 17, no. 5, pp. 3544–3554, May 2021.

- [24] M. Capuzzo, D. Magrin, and A. Zanella, "Confirmed traffic in LoRaWAN: Pitfalls and countermeasures," in *Proc. 17th Annu. Medit. Ad Hoc Netw. Workshop (Med-Hoc-Net)*, Jun. 2018, pp. 1–7.
- [25] J. M. Marais, A. M. Abu-Mahfouz, and G. P. Hancke, "A survey on the viability of confirmed traffic in a LoRaWAN," *IEEE Access*, vol. 8, pp. 9296–9311, 2020.
- [26] K. Adachi, K. Tsurumi, A. Kaburaki, O. Takyu, M. Ohta, and T. Fujii, "Packet-level index modulation for LoRaWAN," *IEEE Access*, vol. 9, pp. 12601–12610, 2021.
- [27] T. Mao, Q. Wang, Z. Wang, and S. Chen, "Novel index modulation techniques: A survey," *IEEE Commun. Surveys Tuts.*, vol. 21, no. 1, pp. 315–348, 1st Quart., 2019.
- [28] K. Tsurumi, A. Kaburaki, K. Adachi, O. Takyu, M. Ohta, and T. Fujii, "Simple clock drift estimation and compensation for packet-level index modulation and its implementation in LoRaWAN," *IEEE Internet Things J.*, vol. 9, no. 16, pp. 15089–15099, Aug. 2022.
- [29] K. Suzuki, K. Adachi, M. Ohta, O. Takyu, and T. Fujii, "Flexible index mapping scheme for packet-level index modulation," *IEEE Wireless Commun. Lett.*, vol. 11, no. 4, pp. 703–706, Apr. 2022.
- [30] *Propagation Data and Prediction Methods for the Planning of Short-Range Outdoor Radiocommunication Systems and Radio Local Area Networks in the Frequency Range 300 MHz to 100 GHz*, document ITU-R P.1411-11, Sep. 2021.
- [31] *920MHz-Band Telemeter, Telecontrol and Data Transmission Radio Equipment*, Standard ARIB STD-T108, Apr. 2021.



Kosuke Suzuki (Member, IEEE) received the B.E. degree in information engineering from the National Institution for Academic Degrees and Quality Enhancement of Higher Education, Tokyo, Japan, in 2021, where he is currently pursuing the M.E. degree.

His current research interests include medium access control layer technologies for massive machine-type communication. He was a recipient of the WPMC Best Student Paper Award in 2020, the IEEJ Tokyo Branch Student Encouragement Award

in 2021, and the IEICE Tokai Section Student Award in 2021.



Koichi Adachi (Senior Member, IEEE) received the B.E., M.E., and Ph.D. degrees in engineering from Keio University, Japan, in 2005, 2007, and 2009, respectively.

From 2007 to 2010, he was a Japan Society for the Promotion of Science (JSPS) Research Fellow. He was a Visiting Researcher at the City University of Hong Kong in April 2009 and a Visiting Research Fellow at the University of Kent from June to August 2009. From May 2010 to May 2016, he was with the Institute for Infocomm Research, A*STAR,

Singapore. He is currently an Associate Professor at The University of Electro-Communications, Japan. His research interests include cooperative communications and energy-efficient communication technologies.

Dr. Adachi is a member of the IEICE. He was recognized as the Exemplary Reviewer from IEEE WIRELESS COMMUNICATIONS LETTERS in 2012, 2013, 2014, and 2015. He was awarded Excellent Editor Award from IEEE ComSoc MMTC in 2013. He is a coauthor of the WPMC2020 Best Student Paper Award. He served as the General Co-Chair for the 10th and 11th IEEE Vehicular Technology Society Asia-Pacific Wireless Communications Symposium (APWCS), the Track Co-Chair for the Transmission Technologies and Communication Theory of the 78th and 80th IEEE Vehicular Technology Conference in 2013 and 2014, respectively, the Symposium Co-Chair for the Communication Theory Symposium of IEEE Globecom 2018, the Tutorial Co-Chair for IEEE ICC 2019, and the Symposium Co-Chair for the Wireless Communications Symposium of IEEE Globecom 2020. He was an Associate Editor of *IET Transactions on Communications* from 2015 to 2017, IEEE WIRELESS COMMUNICATIONS LETTERS since 2016, IEEE TRANSACTIONS ON VEHICULAR TECHNOLOGY from 2016 to 2018, IEEE TRANSACTIONS ON GREEN COMMUNICATIONS AND NETWORKING since 2016, and IEEE OPEN JOURNAL OF VEHICULAR TECHNOLOGY since 2019.



Mai Ohta (Member, IEEE) received the B.E., M.E., and Ph.D. degrees in electrical engineering from The University of Electro-Communications, Tokyo, Japan, in 2008, 2010, and 2013, respectively.

Since 2013, she has been an Assistant Professor with the Department of Electronics Engineering and Computer Science, Fukuoka University. Her research interests include cognitive radio, spectrum sensing, LPWAN, and sensor networks.

Dr. Ohta was a recipient of the Young Researcher's Award from IEICE in 2013.



Osamu Takyu (Member, IEEE) received the B.E. degree in electrical engineering from the Tokyo University of Science, Chiba, Japan, in 2002, and the M.E. and Ph.D. degrees in open and environmental systems from Keio University, Yokohama, Japan, in 2003 and 2006, respectively. From 2003 to 2007, he was a Research Associate with the Department of Information and Computer Science, Keio University. From 2004 to 2005, he was a Visiting Scholar with the School of Electrical and Information Engineering, The University of Sydney.

From 2007 to 2011, he was an Assistant Professor with the Department of Electrical Engineering, Tokyo University of Science. He was an Assistant Professor from 2011 to 2013, an Associate Professor from 2013 to 2023, and has been a Professor since 2023 with the Department of Electrical and Computer Engineering, Shinshu University. His current research interests are in wireless communication systems and distributed wireless communication technology. He was a recipient of the Young Researcher's Award from IEICE 2010, the 2010 Active Research Award in Radio Communication Systems from IEICE Technical Committee on RCS, and the 2018 Best Paper Award in Smart Radio from IEICE Technical Committee on SR.



Takeo Fujii (Senior Member, IEEE) received the B.E., M.E., and Ph.D. degrees in electrical engineering from Keio University, Yokohama, Japan, in 1997, 1999, and 2002, respectively.

From 2000 to 2002, he was a Research Associate with the Department of Information and Computer Science, Keio University. From 2002 to 2006, he was an Assistant Professor with the Department of Electrical and Electronic Engineering, Tokyo University of Agriculture and Technology. From 2006 to 2014, he was an Associate Professor with the Advanced

Wireless Communication Research Center, The University of Electro-Communications. He is currently a Professor and the Director of the Advanced Wireless and Communication Research Center, The University of Electro-Communications. His current research interests include cognitive radio and ad-hoc wireless networks.

Dr. Fujii is a fellow of IEICE. He was a recipient of the Best Paper Award from the IEEE VTC 1999-Fall, the 2001 Active Research Award in Radio Communication Systems from the IEICE Technical Committee of RCS, the 2001 Ericsson Young Scientist Award, the Young Researcher's Award from the IEICE in 2004, the Young Researcher Study Encouragement Award from IEICE Technical Committee of AN in 2009, the Best Paper Award in the IEEE CCNC 2013, and the IEICE Communication Society Best Paper Award in 2016.